 https://doi.org/10.3311/PPch.21723

Periodica Polytechnica Chemical Engineering, 67(2), pp. 296–309, 2023

Pyro-gasification of Rice Husk to Bio-fuel

An Optimization Study of Process Parameters

Tutuk Djoko Kusworo[1*], Andri Cahyo Kumoro[1], Habib Al-Aziz[1], Dani Puji Utomo[1]

[1] Department of Chemical Engineering, Faculty of Engineering, Universitas Diponegoro, Jl. Prof. Sudarto No. 13, Tembalang, 50275 Semarang, Indonesia
[*] Corresponding author, e-mail: tdkusworo@che.undip.ac.id

Received: 20 December 2022, Accepted: 17 March 2023, Published online: 18 May 2023

Abstract

Rice husk is a promising candidate of sustainable biomass-based renewable energy source with a gross caloric content of around 19.73 MJ/kg. As an efficient thermo-conversion process, pyro-gasification has the potential to convert biomass into oil and gas fuels. However, the bio-oil and gas yields are strongly dependent on the pyro-gasification operating parameters. This study employed response surface methodology (RSM) based on central composite design (CCD) experiment to determine the optimum conditions for pyro-gasification of rice-husk. Three selected most influencing operating parameters, namely feed mass (g), nitrogen flow (mL/min), and reactor temperature (°C) were optimized through 16 individual experimental runs for their possible synergistic effects. The results show excellent model fitting criteria (R^2 > 0.9 and R^2-adj > 0.85) for bio-oil and gas product responses that proves the suitability of RSM based on CCD experiment for rice-husk pyro-gasification study. The optimized optimum condition for rice-husk pyro-gasification process was at 897 g of feed mass, 1.97 mL/min of N_2 gas flowrate, and 593 °C of reaction temperature. These conditions allow the achievement of estimated bio-oil and gas product yield of 47.78% and 11.41%, respectively. The composition analysis revealed that the main component of bio-oil was C_{15} (unsaturated), whereas the gas products were C_3–C_4. This study suggests that rice-husk pyro-gasification is capable to achieve maximum yield of bio-oil and gas products with low char generation.

Keywords

biomass, optimization, pyro-gasification, response surface methodology, rice husk

1 Introduction

Nowadays, the world population has been suffering from energy sustainability issue due to the continuous fuel consumption by both industrial and transportation activities. Because petroleum and natural gas that are currently supplying the main world's energy are regarded as non-renewable resources, their reserve will gradually be depleted [1]. Indonesia continues to look for sustainable agricultural residues as potential sources of new renewable energy (NRE). One of the NRE sources is bioenergy derived from biomass, domestic waste, and city waste [2].

The agricultural residues that are abundantly available and renewable can be the promising alternatives to fossil energy sources and have gained remarkable interest from researchers around the world. Indeed, biomass from agricultural residues is one of the best substitutes to fossil resources in various applications, such as heat generation, transportation power, fuel, and chemical and biomaterial production. The use of biomass as an energy source is advantageous, which mainly due to its lower cost, less greenhouse gas emission, high conversion efficiency, and high potential to eradicate environmental issues [3]. The Indonesian Ministry of Energy and Mineral Resources has set policy direction in the energy sector that prioritizes the development and utilization of renewable energy through the utilization of Biofuels.

The increasing demand for sustainable energy supply has attracted researchers to convert agricultural residues, especially rice husks into fuel [4]. Rice husk is a type of biomass that is generated from the rice milling process. Because the shape and size of rice husks are almost uniform, they are very suitable for further processing. Based on their chemical composition, rice husks contain carbon (charcoal substances) 1.33%, hydrogen 1.54%, oxygen 33.64%, and silica (SiO_2) 16.98%. Rice husks have a density of 125 kg/m^3 with a caloric value of 13.81 MJ/kg [5]. This chemical nature means that rice husks can be used as

Cite this article as: Kusworo, T. D., Kumoro, A. C., Al-Aziz, H., Utomo, D. P. "Pyro-gasification of Rice Husk to Bio-fuel: An Optimization Study of Process Parameters", Periodica Polytechnica Chemical Engineering, 67(2), pp. 296–309, 2023. https://doi.org/10.3311/PPch.21723

raw materials for the manufacture of various chemicals as well as a potential source of energy.

Previous study revealed that rice husk is a highly potential raw material for the production of syngas through thermochemical conversion. The thermochemical conversion process converts biomass to other products through the introduction of heat, the use of appropriate catalysts, or chemical reactants [6]. In general, the thermo-chemical conversion by pyrolysis, gasification, and thermal liquefaction are the most widely employed process for producing biofuels and chemicals from biomass [7]. Basically, this thermochemical conversion process results in three different groups of products, namely biochar (solid), bio-oil (liquid), and syngas (gas). These products can be directly used or further processed to produce highly valuable biofuels and renewable chemicals.

First, the combustion process is one of the most straightforward and is easily practiced commercially techniques for converting biomass to generate heat and energy. However, this option is not an environmentally friendly method because it emits greenhouse gases that badly affect sustainable environment. Furthermore, the pyrolysis process is basically a partial combustion using less oxygen from the air to produce gas and liquid products with short carbon chains, and leaving charcoal as the by-product. This process converts biomass through thermochemical mechanism at temperatures at 300–900 °C and ambient pressure in the absence or less existence of air. Therefore, this process results in bio-oil (a mixture of carboxylic acid, ketone, aldehyde, or aromatic), biochar, and syngas (a combination of H_2, CO, CH_4, CO_2) [8]. Pyrolysis process is usually operated at heating rates of 10–50 °C/min under an inert N_2 atmosphere [9]. Previous research found that rice husks pyrolysis in a multimode microwave yielded 21% of bio-oil that contains 60–70% phenolic compounds. In addition, the biochar obtained from pyrolysis account for 25% of pyrolysis products with a caloric value of 25.16 MJ/kg, and being comparable to the lowest grade of coal [10]. The design of process parameters must consider the kinetic reaction behavior that occur in the process. The activation energies of thermochemical conversion process for several biomasses have been studied such as sawdust (59–77 kJ/mol), Plum pits (71–82 kJ/mol), olive pits (69–90 kJ/mol) [11], rose seeds (167–210 kJ/mol) [12], quince waste (44–105 kJ/mol) [13], and rice husk around 150 kJ/mol [14]. The estimated activation energy values can be used to estimate the thermodynamic properties such as Gibbs free energy, enthalpy, and entropy [9]. These kinetic and thermodynamic parameters are helpful in the design and optimization of process parameters.

Gasification is another thermochemical process that involves heating with partial oxidation using oxygen or air at 800–1800 °C [15]. The gasification process produces syngas with a low calorific value (4–7 MJ/kg) that is still suitable for boiler, engine, or turbine applications. But it is expensive [16]. The composition of the gas produced depends on the process condition and the raw materials. Gases produced from lower temperature gasification (below 1000 °C) are rich in carbon monoxide, hydrogen, methane, carbon dioxide, aliphatic hydrocarbons, benzene, toluene, water, and tar. In contrast, the syngas derived from high-temperature gasification (above 1200 °C), is mainly composed of carbon monoxide, hydrogen, carbon dioxide, and water [17].

Currently, the pyro-gasification process has been developed as the combination between pyrolysis and gasification processes [18]. The Pyro-Gasification technology is aimed at the gasification of the biomass while simultaneously also producing biochar. The Pyro-Gasification process can be carried out using either an air/steam or oxygen/steam mixture depending on the application of the resulting syngas. However, the main gases produced in the Pyro-Gasification installations for wood waste and agriculture residue is syngas. The syngas is mostly composed of carbon monoxide, hydrogen, carbon dioxide, nitrogen and some hydrocarbon elements or compound such as methane, ethane, ethylene, propane, sulfur oxides, nitrogen oxides, and ammonia [19]. The carbon monoxide and carbon dioxide are mainly originated from the decomposition and also reforming of carboxyl and carbonyl groups. Light hydrocarbons stemmed from the decomposition of weak methoxy and methylene bonds. Accordingly, hydrogen is the result of the reforming and decomposition of C–H groups and aromatics. Although pyro-gasification technology mainly produces gas and short-chain liquid hydrocarbons suitable for use as fuel, there are also little amounts of long-chain liquid hydrocarbons (crude oil) and residual solid waste. Furthermore, its operating condition is milder than gasification and pyrolysis technology that requires lower operational costs [18]. Considering the above-mentioned matters, this study focuses on the hybrid method that combines pyrolysis and gasification methods to process rice husks.

Although the thermo-conversion process of rice husk into bio-oil has been carried out by several previous researchers [20–22], there is limited study in regard to

the optimization of process parameters of non-catalytic pyro-gasification. This study aimed to investigate the influence of nitrogen flow rate, rice husk weight, and operating temperature on the amount of methane and bio-oil produced from the pyro-gasification process. This study also aimed to optimize the operating conditions to achieve maximum conversion of rice husk through the production of methane (gas) and bio-oil using Response Surface Methodology (RSM) method. The RSM method has been proven to be a powerful experimental design if several factors directly influence the targeted response. The method uses statistics approach to find the interaction and relationship between one or more operating parameters with the targeted response based on the real data collected from a specific arrangement of experiments [23].

2 Materials and experimental methods

2.1 Materials

The rice husks used in this study were obtained from a rice milling factory in Semarang, Indonesia. Rice husks are air-dried to remove external moisture. Prior to the experiment, the rice husks sample was milled using a high-speed rotary cutting plant to obtain a homogeneous particle size of 50 mesh.

2.2 Raw material characterization

The physicochemical characterization of rice husks is highly essential to determine their suitability for use as raw materials to produce syngas and bio-oil. Important biomass properties include calorific value, proximate analysis, and ultimate analysis. In addition, the final analysis is also essential to describe the composition of biomass with the five major elements, namely carbon (C), hydrogen (H), oxygen (O), nitrogen (N), and sulphur (S) content [24]. The compositions of raw rice husk are shown in Table 1.

Table 1 Ultimate and proximate analysis of the rice husk

Parameters	Result	Basis
C	43.80%	Dry
H	7.20%	Dry
O	47.70%	Dry
N	0.98%	Dry
S	0.18%	Dry
Moisture content	10.99%	Dry
Ash content	20.64%	Dry
Volatile matter	57.30%	Dry
Fixed carbon	12.50%	Dry
HHV	13.79 MJ/kg	Dry

2.3 Pyro-gasification process

Fig. 1 illustrates the pyro-gasification reactor used in this work that is already installed in Waste Treatment Laboratory of Chemical Engineering Department, Universitas Diponegoro, Indonesia. Pyro-gasification process is a simultaneous process of pyrolysis and gasification process. Pyrolysis process occurs when biomass is thermally converted into gasses, condensable gas, oxygenated compounds, and biochar as intermediate products. Then the intermediate products are further converted into simpler compounds by gasification process with the presence of small amount of oxygen. In this study, the molar ratio of oxygen/biomass was fixed based on the intrinsic oxygen of biomass and empty space of the reactor. Since biomass was fed into fixed bed retort in the reactor, the oxygen would be released naturally during pyro-gasification process through the particles gap along with injected nitrogen. In the other words, oxygen still existed in the reactor as gasification agent with the flow of nitrogen. Oxygen level in the reactor is minimized by continuously injecting N_2 gas thereby the ratio of oxygen/biomass doesn't exceed 1–1.2 that may initiate combustion reaction. The reactor used in this study is semi-batch fixed bed type pyro-gasifier reactor. The reactor dimension was 20 cm diameter and 40 cm height that was suitable to process 1000 g of material mass. The reactor was equipped with 2000 watt coil heater, jacket insulator, thermocouple, and N_2 gas sparger. The reactor temperature was controlled using automatic on-off feedback controller. The gas product was partially condensed by a pair of 1.5-meter-tall shell and tube vertical condensers with 8 tubes in each.

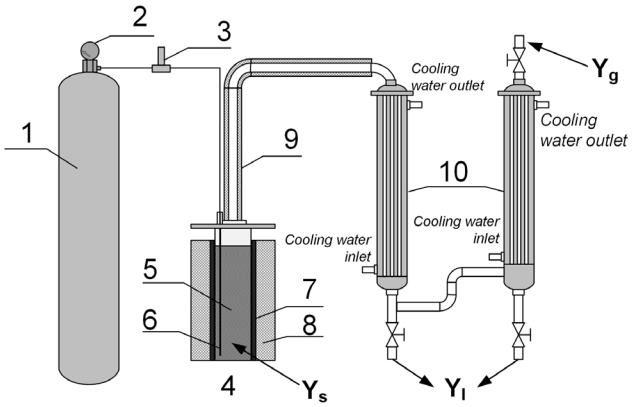

1) N_2 gas bottle; 2) Regulator valve; 3) Rotameter; 4) Reactor; 5) Feed chamber; 6) N_2 gas sparger; 7) Electric heater; 8) Reactor Insulation; 9) Pipe insulation; 10) Condenser; Yg (gas yield); Yl (liquid yield); Ys (solid yield)

Fig. 1 Pyro-gasification reactor

The pyro-gasification began with a careful weighing of rice husk as the feed, and followed by introducing the rice husk into the pyro-gasification reactor of a predetermined mass of feed (800 g, 900 g or 1000 g). Before the pyro-gasification process started, the temperature in the reactor was set according to the desired experimental condition. Then, the reactor was continuously supplied with gaseous nitrogen at a specific flow rate to completely remove the oxygen present in the reactor that potentially burn the rice husk and form ash in the pyro-gasification reactor. Usually, the bio-oil and gas fraction would be produced around 10 minutes after the pyro-gasification process started and last for about 2 hours. The liquid product was collected through bottom side of the condenser (Y_l) and the gas product (Y_g) was sampled via sampling point in uncondensed gas outlet. The solid product (Y_s) was collected after completing the reaction (~2 h) by unmounting the reactor flange and manually cleaned.

2.4 Bio-oil purification

The pyro-gasification process resulted in liquid and gas products that were respectively collected from the bottom and top ends of the condensers. The accumulated liquid product obtained from the pyro-gasification process was mixed with n-hexane to separate the water and bio-oil. Bio-oil yield was calculated as a mass percentage of the biomass feed. Similarly, the charcoal yield was calculated as the mass percentage of the rice husk feed. As for the gas product, the yield was calculated based on the mass balance of rice husk feed, total bio-oil, biochar, and gas. Then, bio-oil and gas products were subjected to chemical component analysis.

2.5 Products characterization

Products characterization by performing Gas Chromatography–Mass Spectroscopy (GC-MS) analysis was conducted to find out the chemical composition of both liquid and gas products. The GC-MS was performed using a Shimadzu GCMS-QP2010 SE, Japan gas chromatography type with a single quadrupole mass spectrometer available in the Central Laboratory of Universitas Diponegoro.

2.6 Experimental design for optimization

The response surface methodology (RSM) combines mathematical and statistical approaches to obtain the most suitable empirical models for a specific correlation. This method requires a careful experimental design to optimize the response (output variable denoted as Y) that is affected by several independent variables (input variables denoted as $X_1, X_2, X_3, \ldots$ etc.) [25]. Therefore, a set of experiments, called run, was performed in which changes were made to input variables to identify the reason for changes in the output response.

The relationship between the response (Y) and the independent variables X_s can be simply written as:

$$Y = f\left(X_1, X_2, \ldots, X_i,\right) + \varepsilon \ , \tag{1}$$

where:
Y = dependent variable
X_i = independent variable/factor (i = 1, 2, 3, …, k)
ε = error.

The first step of RSM is to find a relationship between the Y response and the X-factor through the first-order polynomial equation and used a linear regression model, otherwise known as the first-order model (Eq. (2)):

$$Y = \beta_0 + \sum_{i=1}^{k} \beta_i X_i \ . \tag{2}$$

The design of the first-order experiment with suitable for the factor filter stage is the factorial 2k (Two-Level Factorial Design) design. Furthermore, for the second-order model, there is usually curvature and used second-order polynomial models whose functions are quadratic, according to Eq. (3):

$$Y = \beta_0 + \sum_{i=1}^{k} \beta_i X_i + \sum_{i=1}^{k} \beta_{ii} X_i^2 + \sum \sum_{i<j} \beta_{ij} X_i X_j + \varepsilon \ . \tag{3}$$

The design of the second-order experiment used was the Factorial Three-Level Design, which is suitable for optimization issues. Then from the order II model determined stationary point, characteristics of the response surface, and optimization model.

The statistical model analysis is shown in the Analysis of Variance (ANOVA). This analysis includes Fisher's F-test, which indicates possible $p(F)$ associations, R correlation coefficients, and R^2 determination coefficients that serve to measure regression models. The analysis also includes student's t-value for estimated coefficients and possible $p(t)$ associations. The squared model is presented in contour plots (2D) and surface plots (3D).

Table 2 shows the variable analysis of the following squares:

- SST (Total Sum Square) is the total sum of squares of real deviations from the mean and degree of freedom and measures the spread of all average variants.

$$\mathrm{SST} = \mathrm{SSR} + \mathrm{SSE} \tag{4}$$

Table 2 Variable analysis

Source	Df	Sum of squares	Mean squares	*F*-value
Regression	$p-1$	SSR	SSR/($p-1$)	$\frac{\text{SSR}/(p-1)}{\text{SSR}/(N-p)}$
Residual	$n-p$	SSE	SSE/($N-p$)	
Total	$n-1$	SST		

- SSR (Sum Square Regression) is the sum of squares obtained from regression (a suitable model). It measures deviations whose value can be predicted through a linear relationship between the expected value and the value to be found.

$$\text{SSR} = \sum\left(\dot{Y}_u - \ddot{Y}\right)^2 \tag{5}$$

- SSE (Sum Square Error) calculates the difference in the value found in u^{th} and the predicted value in u^{th}.

$$\text{SSE} = \sum\left(Y_u - \dot{Y}_u\right)^2 . \tag{6}$$

Based on Eqs. (4)–(6), it can be simulated that

$$\text{SST} = \text{SSR} + \text{SSE} = \sum\left(Y_u - \ddot{Y}\right)^2 . \tag{7}$$

The same relationship happens to a degree of freedom. From the sum of squares and degrees of space, we can estimate two variances of σ^2:

$$\sigma^2 = \frac{\sum\left(Y_u - Y\right)^2}{n-1}, \tag{8}$$

where $n-1$ is the degree of freedom. When both SSR and SSE are divided by the degree of freedom they will result in variance values. Thus, the first variance is derived from SSR, whereas the second variance is calculated from the SSE.

$$\begin{aligned}\sigma_1^2 &= \frac{\sum\left(Y_u - Y\right)^2}{p-1} = \frac{\text{SSR}}{p-1} \\ \sigma_1^2 &= \frac{\sum\left(Y_u - Y\right)^2}{n-p} = \frac{\text{SSE}}{n-p}\end{aligned} \tag{9}$$

The *F*-spread or *F*-value is the variance ratio of two estimates, which arise from a typical spread. This means that there is no significant difference between the process experiment and its model. Therefore, the *F*-spread test was used as a test tool to obtain an initial hypothesis (H_0) that showed no difference between the two processes.

$$F = \frac{\text{Mean Square to Regression}}{\text{Mean Square to Residual}} \tag{10}$$

$$F = \frac{\frac{\text{SSR}}{p-1}}{\frac{\text{SSE}}{n-p}} \tag{11}$$

The *F* value obtained from the calculation was then compared with the *F*-value of the reference. Suppose the calculated value is less than the reference value. In that case, the variances can be considered homogeneous, and the H_0 value is accepted, which means the value *F* is in the normal scatter area. On the other hand, if *F* calculation exceeds the *F*-reference value, then the variance is considered significant. Hence, they are called alternative hypothesis (H_1) and reject the initial hypothesis (H_0), which means the value of *F* is outside the normal spread range. Table 3 represents the coded values of independent process variables. The CCD technique consists of axial point ($2k$), factorial points (2^k), and replicates at center points (n_k). Experimental runs according to CCD are presented in Table 4.

ANOVA is used to compare the average population of the population variety. The right type of data for ANOVA is nominal and ordinal on its free variable. If the data on the free variable in the form of intervals or ratios, then it must be changed first in ordinal or nominal form. At the same time, the bound variable is the data interval or ratio.

3 Results and discussion

3.1 TGA analysis of rice husk

The thermogram obtained from thermogravimetric analysis of rice husk sample is presented as weight-loss curve and weight-loss rate curve (DTG) as presented in Fig. 2. Based on its physical phenomenon, the weight loss trend of the samples can be split into three different stages. The first stage is weight loss due to the vaporization of moisture and other volatile compounds that occurs at temperature range ambient temperature to around 200 °C. Meanwhile, the second stage represents the release of light hydrocarbons and depolymerization of complex biopolymers at about 200 to 400 °C that results in low molecular hydrocarbons. At this stage, the heat supplied was sufficient to break-down the chemical bonds within the

Table 3 Coded variables of experimental process parameters using CCD technique

Independent process variable	Coded levels		
	−1	0	1
Feed mass, (g)	880	900	920
Nitrogen flowrate, (mL/min)	1.80	2.00	2.20
Reactor temperature, (°C)	590	594	598

Table 4 Experimental design of pyro-gasification process

Standard run	Variable		
	N_2 flow (L/min)	Temperature (°C)	Biomass weight (gram)
1	1.80	590.00	880.00
2	2.20	590.00	880.00
3	1.80	590.00	950.00
4	2.20	590.00	950.00
5	1.80	598.00	880.00
6	2.20	598.00	880.00
7	1.80	598.00	920.00
8	2.20	598.00	920.00
9	2.00	587.27	900.00
10	2.00	600.73	900.00
11	2.00	500.00	866.36
12	2.00	594.00	933.64
13	1.66	594.00	900.00
14	2.34	594.00	900.00
15	2.00	594.00	900.00
16	2.00	594.00	900.00

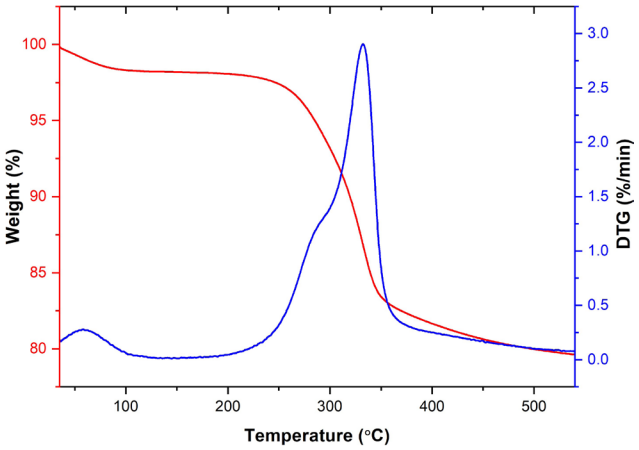

Fig. 2 TG/DTG curves of rice husk thermal decomposition at room temperature to 550 °C

complex biopolymers structure. The third stage is partial decomposition of lignin and char. Finally, the complex organic substances are partially decomposed into carbonaceous materials and leaving the inorganic materials. Therefore, pyrolysis process produced water vapor during the first 10 minutes as the gas product and then followed by the degradation of xylan part of hemicellulose to produce carbon monoxide and carbon dioxide. This result is in good agreement with previous report [26]. In the second stage, the volatile short-chain hydrocarbons, such as methane to butane are produced from the decomposition of hemicellulose, cellulose, and lignin. Furthermore, the longer-chain hydrocarbons (C_8–C_{20}) are produced in the form of bio-oils at the end of second stage following the increased temperature. At the third stage, which the temperature is higher, complex hydrocarbons were decomposed and resulted in light hydrocarbons. In addition, lignin was further carbonized and produced coke residue. The sharp peak observed at 220–380 °C in the DTG curve indicates the major decomposition of rice husks sample. Heat and mass transfer could affect the global decomposition of the process for large particle size. In this study, the rice husk was grinded and sieved using 100 mesh that gave average particle size of 100 µm. According to previous study by Fernandez et al. [11], heat transfer and intra-particle diffusion limitation are negligible for biomass particle of size below 300 µm.

3.2 Pyro-gasification results

The yields of bio-oil and gas of the rice husk pyro-gasification attained from 16 different operating conditions are presented in Table 5. The bio-oil yields ranged from 19–47% by weight, whereas gas yields varied from 6–37% by weight. As discussed in the previous section, the rice husks decomposed at temperatures about 220–400 °C. In this experiment, the pyro-gasification temperature was set 590–600 °C, which was close to the carbonization stage temperature. The results suggested that the product yields variations were highly influenced by the operating

Table 5 Experimental fractional yields of bio-oil and gas product

Run	Responses	
	Bio-oil yield (%)	Gas yield (%)
1	42.61	13.54
2	28.76	7.21
3	21.46	17.62
4	27.22	18.94
5	28.76	32.05
6	24.45	25.95
7	19.21	20.22
8	37.11	9.11
9	22.33	18.85
10	26.80	37.01
11	35.50	27.20
12	31.15	15.55
13	38.56	6.15
14	42.12	1.65
15	47.20	13.49
16	46.90	12.30

conditions. The nitrogen that was continuously flown into the reactor acts as a carrier where at higher flow rate will shorten the retention time of the produced hydrocarbons and leads to a higher heavy hydrocarbons product fraction. Additionally, temperature also played important role in pyro-gasification through thermal decomposition of long-chain hydrocarbons that eventually increased the gas product yields. Since the pyro-gasification process was operated under semi-batch mode, the feed mass also provided considerable effect to the product yield. A higher feed mass leads to a shorter retention time of the evaporated hydrocarbons in the reactor that promotes the attainment of heavy hydrocarbons in the liquid product.

3.3 Bio-oil product optimization

The statistics software automatically generated the best fit model based on the bio-oil yield as the response. The coefficient fitting determination, R^2-values, F-values, and p-values are also presented for the evaluation of fitting model. In this study, the response and independent variables were fitted to each other through a multiple regression. The best fitted model that describes the single and combined effects of operating parameters as the independent variables towards bio-oil yield product is given in Eq. (12):

$$\begin{aligned} Y_{\text{oil}} &= 0.4736 - 0.0393X_1 + 0.0168X_2 - 0.0044X_3 \\ &-0.1118X_1^2 - 0.0623X_2^2 - 0.1738X_3^2 + 0.1046X_1X_2 , \\ &+0.0645X_1X_3 + 0.0542X_2X_3 \end{aligned} \quad (12)$$

where Y_{oil} is the response (bio-oil yield) and X_1, X_2, and X_3 are the coded terms for the selected operating variables, namely the feed mass (X_1), N_2 gas flowrate (X_2) and reactor temperature (X_3). The synergistic effect is indicated by positive value of the constant in the model, while the antagonistic effect is shown by a negative value of the constant for the corresponding independent variable. The fitting criteria shows R^2 = 0.9509 and R^2-adj = 0.8772 indicating the model has a good fit with the experimental data. According to the model, nitrogen flowrate gives synergistic effect to the bio-oil yield. It could be due to the role of nitrogen as the carrier gas where its higher value shortened the resident time of hydrocarbon vapor in the reactor, thereby a higher bio-oil yield can be obtained.

From the Table 6, it is confirmed that the quadratic term of feed mass (X_1) significantly influences the bio-oil yield as indicated by a high F-value of 28.48 and p-value <0.05 (0.0018). In addition, the quadratic terms of both nitrogen flowrate (X_2) and reactor temperature (X_3) also exhibited high F-value of 8.83 and 68.76, respectively. These results indicate that the three operating parameters give significant effect on the bio-oil yield in quadratic terms. However, not all variables give significant direct linear effect on the bio-oil yield. The interaction of feed mass and nitrogen flowrate (X_1X_2) significantly affected to the bio-oil yield by giving high F-value of 21.30. It suggests that feed mass and nitrogen are the important parameters in controlling the production of bio-oil from rice husk pyro-gasification. In this work, both feed mass and nitrogen flow are correlated with the hydrocarbon vapor resident time in the reactor.

Table 6 ANOVA for the regression model and respective model term for bio-oil yield

Source	SS	df	MS	F-value	p-value	Remarks
X_1	0.0053	1	0.0053	5.2067	0.0626	
X_1^2	0.0290	1	0.0290	28.4847	0.0018	Significant
X_2	0.0010	1	0.0010	0.9509	0.3671	
X_2^2	0.0090	1	0.0090	8.8276	0.0249	Significant
X_3	0.0001	1	0.0001	0.0651	0.8071	
X_3^2	0.0700	1	0.0700	68.7573	0.0002	Significant
X_1X_2	0.0219	1	0.0219	21.4957	0.0036	Significant
X_1X_3	0.0083	1	0.0083	8.1830	0.0288	Significant
X_2X_3	0.0059	1	0.0059	5.7811	0.0530	
Error	0.0061	6	0.0010			
Total SS	0.1242	15				

Fig. 3 exhibits the relationship between the process variables and bio-oil yield of in the form of 3D surface and contour plot. The surface plot of three process variables against bio-oil yield response formed dome-like surface with the optimum region is indicated by the dark-red color. As shown in the diagram, the bio-oil yield increased non-linearly until the achievement of an optimum point. It was statistically proven with high F-value and low p-value ($p < 0.05$) as presented in ANOVA result. Fig. 3 (a) clearly demonstrates the elevation of both feed mass and temperature promoted the increase in the bio-oil yield a maximum value. However, bio-oil yield decreased as both operating parameters increased further. These results are in accordance with previous study where the pyrolysis oil yield increased with the increasing of temperature and retention time [27]. In the semi-batch process, the amount of feed mass can be directly correlated with vapor retention time in the pyro-gasification reactor. A higher feed mass inside reactor will consequently cause a shorter retention time of the volatile organic matter inside the reactor. The increase of temperature at bellow center point favors the formation of condensable organic hydrocarbons from biomass due to

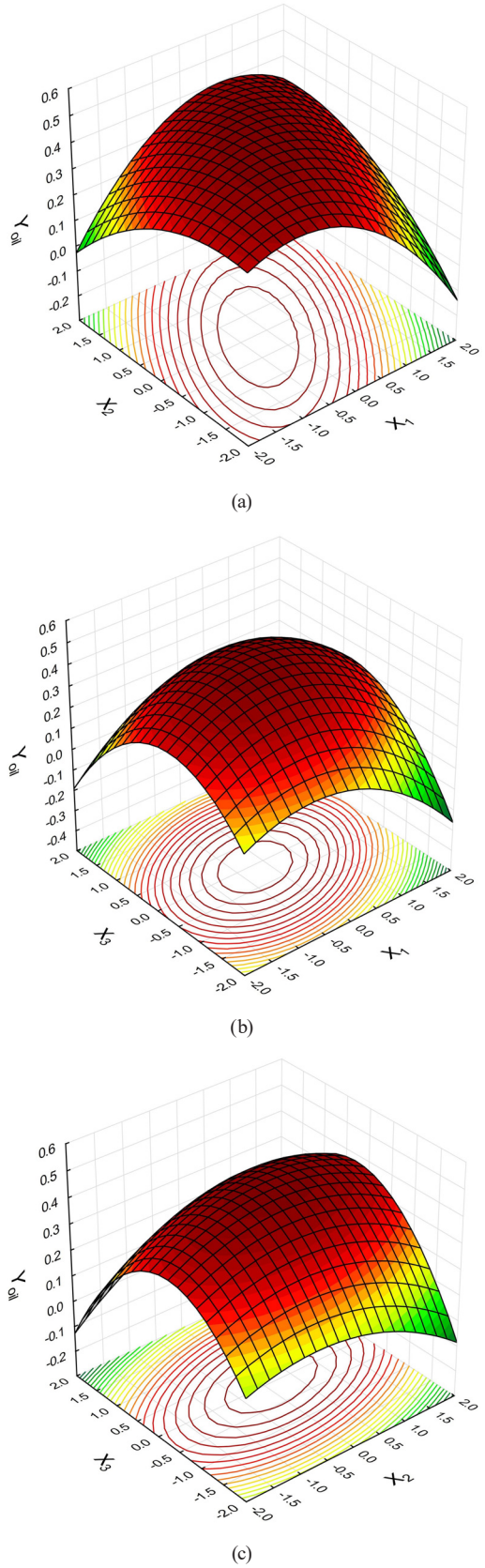

(a)

(b)

(c)

Fig. 3 Surface 3D and contour plot of bio-oil yield response (a) effect of feed mass and N_2 flowrate, (b) effect of feed mass and temperature, and (c) effect of N_2 flowrate and temperature

thermal cracking. However, further increase in temperature leads to the formation of more volatile compounds. As presented in Fig. 3 (b) and (c), high bio-oil yields were obtained at all nitrogen flowrate, indicating that the gas flowrate did not play significant effect on the bio-oil yield.

The correlation between experimental values and predicted values of bio-oil yield is shown in Fig. 4. The predicted value is represented by a straight red line, while the experimental data is represented by the discrete points. It is very obvious that both observed and predicted values of bio-oil yield are very close. Hence, the proposed model represents the pyro-gasification process to produce bio-oil very well. Based on the coefficient of determination (R^2) value, ones can be informed that 95.09% sample variations of bio-oil yield are associated with the independent variables and the rest 4.91% of total variations could not be explained by the model. Theoretically, an excellent mathematics correlation between the independent variables can be justified by a higher correlation coefficient value for all responses.

3.4 Gas product optimization

The experimental results in term of gas product yield responses were fitted to the proposed quadratic model (Eq. (13)). Equation (13) confirms that the linear terms of feed mass (X_1) and nitrogen flowrate (X_2) gave antagonistic effect towards gas yield. As discussed in the previous section, feed mass and nitrogen flowrate are directly correlated with volatile organic compounds retention time in the pyro-gasification reactor. Therefore, a shorter retention time will promote a higher tendency to produce more condensable products (bio-oil) rather than gas products. However, the quadratic terms of feed mass give positive

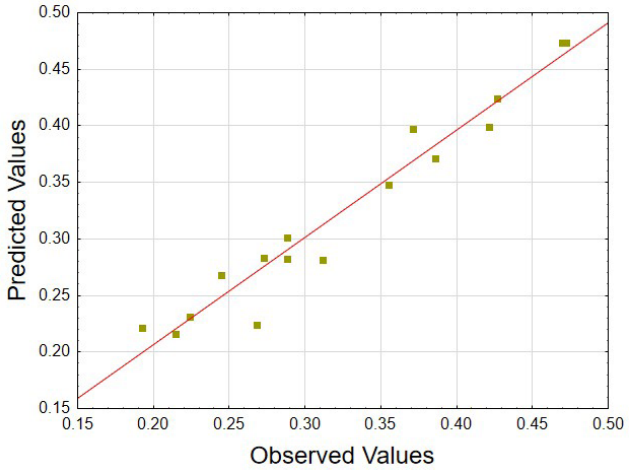

Fig. 4 Predicted value vs observed value plot of bio-oil response

sign indicating its synergetic effect to the gas product. Meanwhile, the reactor temperature shows synergetic effect as proven by the positive sign for both linear and quadratic terms in the model. Higher reactor temperature leads to a higher gas product and a lower tar product due to the intensified thermal cracking of biomass. These results are also in good agreement with the previous studies [28, 29].

$$Y_{gas} = 0.1289 - 0.0475X_1 - 0.0436X_2 + 0.0887X_3 + 0.0602X_1^2 - 0.0634X_2^2 + 0.1066X_3^2 + 0.0066X_1X_2 - 0.1111X_1X_3 - 0.0305X_2X_3 \quad (13)$$

Table 7 presents the ANOVA study of the proposed model to find the significance of independent variables towards gas product response. The significance of the model was verified based on the Fischer test (*F*-value) and probability test (*p*-value). A higher *F*-value and low *p*-value ($p < 0.05$) show the greater reliability of the model and effect significance of the independent variables. According to ANOVA result of gas yield from the rice husk pyrolysis, only interaction parameters of feed mass and temperature (X_1X_3) and nitrogen flowrate and temperature (X_2X_3) exhibited low *F*-value of 0.1080 and 2.3259, respectively as well as high *p*-value of 0.7537 and 0.1781, respectively. Therefore, these independent variable interactions are considered to be not significantly affect the variation of gas yield.

Fig. 5 presents the 3D response surface plot that relates interaction of the involving independent variables. These plots are very useful to analyze the response behavior as the function of the involving process variables through the surface shapes. As clearly seen in Fig. 5, all surface plots

Table 7 ANOVA for the regression model and respective model term for gas fractional yield

Source	SS	df	MS	*F*-value	*p*-value	Remarks
X_1	0.0077	1	0.0077	9.6436	0.0210	Significant
X_1^2	0.0084	1	0.0084	10.5021	0.0177	Significant
X_2	0.0065	1	0.0065	8.1250	0.0292	Significant
X_2^2	0.0093	1	0.0093	11.6265	0.0143	Significant
X_3	0.0269	1	0.0269	33.5910	0.0012	Significant
X_3^2	0.0263	1	0.0263	32.8995	0.0012	Significant
X_1X_2	0.0001	1	0.0001	0.1080	0.7537	
X_1X_3	0.0247	1	0.0247	30.9278	0.0014	Significant
X_2X_3	0.0019	1	0.0019	2.3259	0.1781	
Error	0.0048	6	0.0008			
Total SS	0.1387	15				

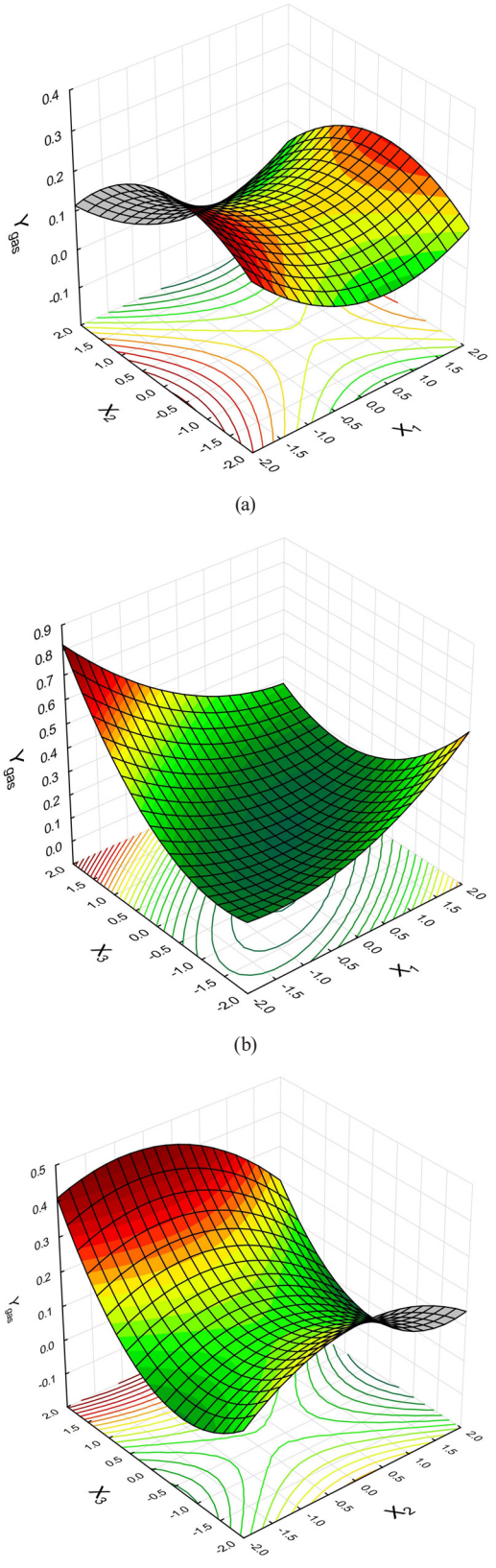

(a)

(b)

(c)

Fig. 5 Surface 3D and contour plot of gas product yield response (a) effect of feed mass and N_2 flowrate, (b) effect of feed mass and temperature, and (c) effect of N_2 flowrate and temperature

show saddle shapes instead of dome-like shape. Saddle-shaped surface has a hyperbolic contour type with a stationary point or saddle point that is neither a maximum nor minimum point. According to Fig. 5 (a), the increasing of feed mass below saddle point caused a decrease in the gas yield due to the shortened retention time. At higher feed mass, the gas product start increased due to more biomass feedstock supplied. A similar trend was also exhibited by temperature effect (Fig. 5 (b) and (c)) where at below saddle point, the increase in temperature led to reduce the gas product yield. This observation could be due to vaporization of the free and bound moisture and volatile organic compounds at low temperature. Subsequently, the elevation of temperature promoted biomass decomposition into condensable organic compounds (bio-oil yield) thereby decreasing the gas yield. However, further rise in temperature resulted in a significant increase in the gas product yield that primarily due to the occurrence of secondary reactions such as decarboxylation, decarbonylation, reforming reactions, depolymerization, etc. Presumably, these secondary reactions resulted in the higher amount non-condensable gases. A similar phenomenon was also reported by Gupta and Mondal [30] where at higher temperature >550 °C the non-condensable gas yield continuously increased due to faster devolatilization reaction along with the reduction of bio-char residue.

The graphical illustration of the observed value versus predicted value of gas yield responses is depicted in Fig. 6. The observed of gas yield varied between 1.65% and 37.01%. Fig. 6 exhibits that the observed gas yield data are very close with those predicted values presented as red line. This result suggests that the model possesses a high accuracy to predict the gas yield. The coefficient of determination (R^2) value is 0.9654 describing that 96.54% of the response variations are influenced by process variables and the 3.46% of total variations could not be explained by the model. The adjusted R^2 value is 0.9316 that further advocates for a high accuracy of the model.

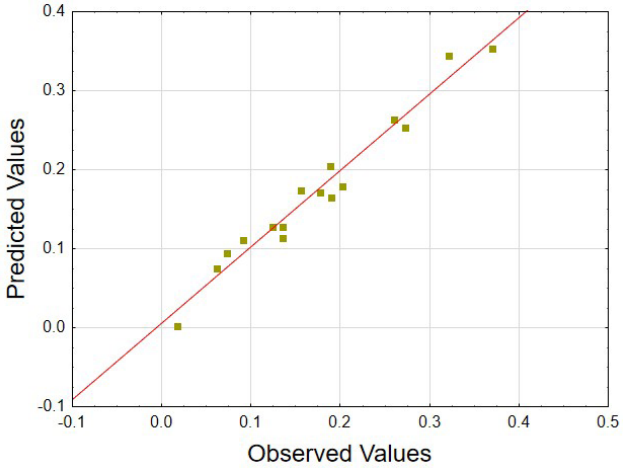

Fig. 6 Predicted value vs observed value plot of gas product response

3.5 Optimization analysis

The multiple objectives consisted of bio-oil and gas yields were optimized by taking into consideration all influencing parameters using Statistica Software V12.5.192.7 [31]. The ultimate objective of this study was to determine the optimum process parameters to produce highest bio-oil product from rice husk pyro-gasification. The overall analyzed ranges of three independent variables and two responses were evaluated to achieve the optimization target. The critical values according to the software analysis were 897 g of feed mass, 1.97 mL/min of nitrogen flowrate, and 593 °C of reactor temperature. These optimum operating conditions gives predicted bio-oil and gas product yields of 47.78% and 11.41%, respectively. The comparison of the result of this study with previous reports is presented in Table 8 [30, 32–37].

3.6 Bio-oil composition analysis

Table 9 exhibits the of hydrocarbon components identified in the bio-oil derived from rice husk through GC-MS analysis. It is clearly seen in Table 9, rice husks pyro-gasification process produced bio-oil containing numerous hydrocarbons fractions. The percentage of peak area (%) for each identified compound demonstrates its relative mass percentage in the bio-oil.

Based on the results of the GC-MS test tabulated in the Table 9, the major compounds identified in bio-oil are classified as long-chain alkanes that amounting to 66.98%.

Table 8 Bio-oil yield at optimized process parameters of previous studies

Biomass	Bio-oil yield (wt%)	Optimization tool	References
Saccharum munja grass	46.00	RSM based CCD	[32]
Pine needles	51.11 51.70	RSM ANN	[30]
HDPE waste	78.70	RSM based FCCD	[33]
Napier grass	50.57	RSM based CCD	[34]
Sagwan sawdust	48.70	RSM based BBD	[35]
Neem press seed cake	52.10	RSM based BBD	[36]
Euphorbia rigida	35.30	RSM based CCD	[37]
Rice husk	47.78	RSM based CCD	This work

Table 9 Chemical composition of bio-oil from rice husk pyro-gasification according to the GC-MS analysis

No.	Compound name	Molecule formula	Mole fraction (%)
1	Pentadecane	$C_{15}H_{32}$	21.00
2	Tetradecane	$C_{14}H_{30}$	9.24
3	Tridecane	$C_{13}H_{28}$	7.28
4	Hexadecane	$C_{16}H_{34}$	6.78
5	1-Tridecene	$C_{13}H_{26}$	6.49
6	1-Tridecanol	$C_{13}H_{28}O$	5.90
7	Dodecane	$C_{12}H_{26}$	4.50
8	Undecane	$C_{11}H_{24}$	3.60
9	Nonane	$C_{9}H_{20}$	3.18
10	1-Tetradecanol	$C_{14}H_{30}O$	2.93
11	Decane	$C_{10}H_{22}$	2.90
12	1-Dodecene	$C_{12}H_{24}$	2.89
13	n-Hexadecanoic acid	$C_{16}H_{32}O_{2}$	2.63
14	Cyclopropane, Nonyl	$C_{12}H_{24}$	2.28
15	9-Octadecenal	$C_{18}H_{34}O$	2.11
16	Hexadecanoic acid, 2 hydroxy-1,3-popanediyl ester	$C_{35}H_{68}O_{5}$	1.84
17	Toluene	$C_{7}H_{8}$	1.83
18	Oleic Acid	$C_{18}H_{34}O_{2}$	1.79
19	1-Decene	$C_{10}H_{20}$	1.73
20	1-Hexadecanol	$C_{16}H_{34}O$	1.56
21	Heptane, 2,4-dimethyl	$C_{9}H_{20}$	1.50
22	Heptane	$C_{7}H_{16}$	0.96
23	Phenol, 2-ethyl	$C_{8}H_{10}O$	0.93
24	1-Nonadecene	$C_{19}H_{38}$	0.91
25	Cyclopentadecane	$C_{15}H_{30}$	0.87
26	9-Borabycyclo, Nonane, 9-hydroxy	$C_{8}H_{15}BO$	0.84
27	1-Heptene	$C_{7}H_{14}$	0.84
28	3-Eicosene	$C_{20}H_{40}$	0.72

In addition, other compounds were also present, such as phenolic compounds 13.43%, long-chain alkenes 11.53%, esters 4.47%, toluene or methyl benzene 1.83%, and acid compound which is just oleic acid is 1.79%.

In this study, rice husks pyro-gasification produced complex mixtures of hydrocarbons because they contained cellulose, hemicellulose, lignin and other extractable compounds that can react through the thermal cracking. The cellulose and hemicellulose contents in rice husks were respectively 25–35% (w/w) and 18–21% (w/w). Meanwhile, lignin and minerals contents in rice husks were 26–31% (w/w) and 15–17% (w/w), respectively [38]. The primary products of cellulose and hemicellulose decomposition were condensable vapors (bio-oil) and gas, whereas lignin decomposition mainly resulted in bio-oil, non-condensable gases, and solid (char) [39].

Among the compounds listed in Table 9, the aliphatic hydrocarbon compounds were mainly composed of alkanes and alkenes, which are well-known to be the main constituents of fossil fuels. Aliphatic hydrocarbons are of great importance in fuel applications. When the temperature raises from 450 °C to 650 °C, the relative content of the aliphatic hydrocarbon compounds gradually increased and reached a maximum of 13.58% at 650 °C. In this case, the temperature range 500–600 °C that major compound long-chain alkanes 66.98% and long-chain alkenes 11.53% [40].

The formation of alkanes and alkenes can be attributed to the generation of an RCOO radical through triglyceride cleavage and followed by decarboxylation. The formation of aromatic compounds is supported by Diels–Alder ethylene addition of a conjugated diene and carboxylic acids that are most likely formed through the cleavage of glycerol moiety [41]. The yields of hydrocarbons as useful chemicals contained in bio-oil are also expected to be increased for the attainment of bio-oils of desirable quality [42].

The second major compound in this result is phenolic compound. Akalın et al. [43] found that phenolic compounds such as tridecanol, tetradecanol, hexadecanol, phenol, and octadecenal can also be formed from the decomposition of furfural and furfural derivatives. They also reported that the content of phenolic compounds increased with an increase in the temperature. Besides, Liu et al. [44] reported that phenolic compounds can also be formed from the degradation of the lignin component in risk husk (by cleavage of the aryl ether linkages in lignin). The basic unit of lignin is the phenyl propane (substituted), which is a rich source of phenolic compounds in the liquid hydrocarbons [45].

A large quantity of esters was obtained from the liquefaction of rice husk with phenolic compound, which may be ascribed to the esterification reactions between fatty acid and phenolic compound in rice husk. Fatty acid can also be partly degraded through decarboxylation at hydrothermal conditions to form various long-chain hydrocarbons [39].

3.7 Gas product composition analysis

The rice husks pyro-gasification process of produces gas, which contains a complex mixture of hydrocarbons as analyzed with GC-MS. The details of hydrocarbon components in the gas product are presented in Table 10.

Table 10 Chemical composition of gas from rice husk pyro-gasification according to the GC-MS analysis

No.	Compound name	Molecule formula	Mol (%)
1	1-Propene	C_3H_6	24.42
2	2-Butene	C_4H_8	24.42
3	1-Pentene	C_5H_{10}	18.11
4	Cyclopentene	C_5H_8	3.28
5	2-Propanol	C_3H_4O	18.66
6	Butyl cyclobutane	C_8H_{16}	5.43
7	Hexane	C_6H_{14}	3.61
8	Cyclopropane, dimethyl	C_5H_{10}	2.07

Based on the GC-MS results presented in the Table 10, most compounds are identified as condensable gas, such as alkenes 70.23%, phenolic compounds 18.66% and alkanes 11.11%. Linear alkanes and alkenes are well-known products derived from direct deoxygenation of the fatty acid feed or the cracking of deoxygenated hydrocarbon product through free radical mechanism. In addition, phenolic compounds are formed from the degradation of the lignin component in risk husk through the cleavage of the aryl ether linkages in lignin structure [44].

Although the gas produced is condensable gas, but it obtained in the gas sampling point. It could be due to the condensing system couldn't accommodate the complete condensation process. It may also as a consequence of the inappropriate nitrogen flow rate, the inlet temperature of cooling water, available heat transfer area, and gas residence time in the condensing zone of the condenser. This phenomenon supports the reason why bio-oil yield achieved in this study was far below the bio-oil yield reported in the previous study.

4 Conclusion

In this study, the pyro-gasification process of rice husk and the optimization of process parameters have been studied in a semi-batch fixed bed reactor. The characterization of rice husk has shown the potential energy utilization up to 13.79 MJ/kg. The rice husk pyro-gasification exhibited three stages of decomposition: moisture evaporation, light hydrocarbon release from biopolymer decomposition, and decomposition of lignin and char. The developed RSM models exhibited high determination coefficient and high significance parameter values indicating the model strongly represented the experimental data. The predicted optimum conditions were 897 g for feed mass, 1.97 mL/min for N_2 gas flowrate, and 593 °C for reactor temperature, resulting in bio-oil yield and gas yield of 47.78% and 11.41%, respectively. The statistical analysis indicates that reactor temperature is the most important factor that control product distribution. But N_2 flowrate and feed mass are influential factors for affecting residence time and energy consumption in the process. The main composition of bio-oil was paraffinic hydrocarbon (C_{15} up to 21%) and the main composition of gas product was petroleum hydrocarbon gas (C_4 up to 24%). Thus, it may be concluded that the pyro-gasification of rice husk potentially produce biofuel at a commercial scale due to its improved overall sustainability.

Acknowledgement

This research was fully funded by Universitas Diponegoro through International Publication Research (RPI) Research Grant Scheme with a contract No. 569-163/UN7/D2/PP/VII/2022.

References

[1] Wicker, R. J., Kumar, G., Khan, E., Bhatnagar, A. "Emergent green technologies for cost-effective valorization of microalgal biomass to renewable fuel products under a biorefinery scheme", Chemical Engineering Journal, 415, 128932, 2021. https://doi.org/10.1016/j.cej.2021.128932

[2] Afandi, R., Aryatie, W., Puspitasari, D. E., Mirayanti, B. A. "Balitbang: Transformasi & Inovasi, Dukung Sektor Energi Nasional" (R&D: Transformation & Innovation to Support National Energy Sector), [pdf] Jurnal Energi Media Komunikasi Kementerian Energi dan Sumber Daya Mineral, 2, pp. 9–25, 2018. Available at: https://www.esdm.go.id/assets/media/content/content-jurnal-energi-edisi-ii-tahun-2018.pdf [Accessed: 01 November 2022] (in Indonesian)

[3] Guedes, R. E., Luna, A. S., Torres, A. R. "Operating parameters for bio-oil production in biomass pyrolysis: A review", Journal of Analytical and Applied Pyrolysis, 129, pp. 134–149, 2018. https://doi.org/10.1016/j.jaap.2017.11.019

[4] Quispe, I., Navia, R., Kahhat, R. "Energy potential from rice husk through direct combustion and fast pyrolysis: A review", Waste Management, 59, pp. 200–210, 2017. https://doi.org/10.1016/j.wasman.2016.10.001

[5] Zurairah, M., Saragih, E. S., Misdawati, M. "Comparison Of Thermo Gravimetric Characterization Of Active Carbon Analyzer Rice Husk With Rice Husk Implementation", Jurnal Matematika Dan Ilmu Pengetahuan Alam LLDikti Wilayah 1 (JUMPA), 1(2), pp. 64–68, 2021. https://doi.org/10.54076/jumpa.v1i2.176

[6] Xu, J., Jiang, J., Zhao, J. "Thermochemical conversion of triglycerides for production of drop-in liquid fuels", Renewable and Sustainable Energy Reviews, 58, pp. 331–340, 2016. https://doi.org/10.1016/j.rser.2015.12.315

[7] Ahmad, F. B., Zhang, Z., Doherty, W. O. S., O'Hara, I. M. "The outlook of the production of advanced fuels and chemicals from integrated oil palm biomass biorefinery", Renewable and Sustainable Energy Reviews, 109, pp. 386–411, 2019. https://doi.org/10.1016/j.rser.2019.04.009

[8] Li, J., Dou, B., Zhang, H., Zhang, H., Chen, H., Xu, Y., Wu, C. "Pyrolysis characteristics and non-isothermal kinetics of waste wood biomass", Energy, 226, 120358, 2021. https://doi.org/10.1016/j.energy.2021.120358

[9] Al-Rumaihi, A., Parthasarathy, P., Fernandez, A., Al-Ansari, T., Mackey, H. R., Rodriguez, R., Mazza, G., McKay, G. "Thermal degradation characteristics and kinetic study of camel manure pyrolysis", Journal of Environmental Chemical Engineering, 9(5), 106071, 2021. https://doi.org/10.1016/j.jece.2021.106071

[10] Salema, A. A., Ani, F. N. "Pyrolysis of oil palm empty fruit bunch biomass pellets using multimode microwave irradiation", Bioresource Technology, 125, pp. 102–107, 2012. https://doi.org/10.1016/j.biortech.2012.08.002

[11] Fernandez, A., Soria, J., Rodriguez, R., Baeyens, J., Mazza, G. "Macro-TGA steam-assisted gasification of lignocellulosic wastes", Journal of Environmental Management, 233, pp. 626–635, 2019. https://doi.org/10.1016/j.jenvman.2018.12.087

[12] Torres-Sciancalepore, R., Asensio, D., Nassini, D., Fernandez, A., Rodriguez, R., Fouga, G., Mazza, G. "Assessment of the behavior of *Rosa rubiginosa* seed waste during slow pyrolysis process towards complete recovery: Kinetic modeling and product analysis", Energy Conversion and Management, 272, 116340, 2022. https://doi.org/10.1016/j.enconman.2022.116340

[13] Torres-Sciancalepore, R., Fernandez, A., Asensio, D., Riveros, M., Fabani, M. P., Fouga, G., Rodriguez, R., Mazza, G. "Kinetic and thermodynamic comparative study of quince bio-waste slow pyrolysis before and after sustainable recovery of pectin compounds", Energy Conversion and Management, 252, 115076, 2022. https://doi.org/10.1016/j.enconman.2021.115076

[14] Chen, C., Qu, B., Wang, W., Wang, W., Ji, G., Li, A. "Rice husk and rice straw torrefaction: Properties and pyrolysis kinetics of raw and torrefied biomass", Environmental Technology & Innovation, 24, 101872, 2021. https://doi.org/10.1016/j.eti.2021.101872

[15] Awalludin, M. F., Sulaiman, O., Hashim, R., Nadhari, W. N. A. W. "An overview of the oil palm industry in Malaysia and its waste utilization through thermochemical conversion, specifically via liquefaction", Renewable and Sustainable Energy Reviews, 50, pp. 1469–1484, 2015. https://doi.org/10.1016/j.rser.2015.05.085

[16] Maity, S. K. "Opportunities, recent trends and challenges of integrated biorefinery: Part I", Renewable and Sustainable Energy Reviews, 43, pp. 1427–1445, 2015. https://doi.org/10.1016/j.rser.2014.11.092

[17] Samiran, N. A., Jaafar, M. N. M., Ng, J.-H., Lam, S. S., Chong, C. T. "Progress in biomass gasification technique - With focus on Malaysian palm biomass for syngas production", Renewable and Sustainable Energy Reviews, 62, pp. 1047–1062, 2016. https://doi.org/10.1016/j.rser.2016.04.049

[18] Lajili, M., Guizani, C., Escudero Sanz, F. J., Jeguirim, M. "Fast pyrolysis and steam gasification of pellets prepared from olive oil mill residues", Energy, 150, pp. 61–68, 2018. https://doi.org/10.1016/j.energy.2018.02.135

[19] Zhang, Y., Zhao, Y., Gao, X., Li, B., Huang, J. "Energy and exergy analyses of syngas produced from rice husk gasification in an entrained flow reactor", Journal of Cleaner Production, 95, pp. 273–280, 2015. https://doi.org/10.1016/j.jclepro.2015.02.053

[20] Das, S., Goud, V. V. "RSM-optimised slow pyrolysis of rice husk for bio-oil production and its upgradation", Energy, 225, 120161, 2021. https://doi.org/10.1016/j.energy.2021.120161

[21] Gautam, N., Chaurasia, A. "Study on kinetics and bio-oil production from rice husk, rice straw, bamboo, sugarcane bagasse and neem bark in a fixed-bed pyrolysis process", Energy, 190, 116434, 2020. https://doi.org/10.1016/j.energy.2019.116434

[22] Qiu, Z., Zhai, Y., Li, S., Liu, X., Liu, X., Wang, B., Liu, Y., Li, C., Hu, Y. "Catalytic co-pyrolysis of sewage sludge and rice husk over biochar catalyst: Bio-oil upgrading and catalytic mechanism", Waste Management, 114, pp. 225–233, 2020. https://doi.org/10.1016/j.wasman.2020.07.013

[23] Montgomery, D. C. "Response Surface Methods and Designs Chapter 11", In: Design and Analysis of Experiments, Wiley, 2008, pp. 478–553. ISBN 9780470128664

[24] Jimoh, A. O., Namadi, M. M., Ado, K., Muktar, B. "Proximate and Ultimate Analysis of *Eichornia natans* (Water Hyacinth), *Pistia stratiotes* (Water Lettuce) and *Nymphaea lotus* (Water Lily) in the Production of Biofuel", Advanced in Applied Science Research, 7(4), pp. 243–249, 2016.

[25] Zalazar-Garcia, D., Román, M. C., Fernandez, A., Asensio, D., Zhang, X., Fabani, M. P., Rodriguez, R., Mazza, G. "Exergy, energy, and sustainability assessments applied to RSM optimization of integrated convective air-drying with pretreatments to improve the nutritional quality of pumpkin seeds", Sustainable Energy Technologies and Assessments, 49, 101763, 2022. https://doi.org/10.1016/j.seta.2021.101763

[26] Xu, G., Cai, X., Wang, L., Zhang, Q., Fang, B., Zhong, X., Yao, J. "Thermogravimetric-infrared analysis and performance optimization of co-pyrolysis of oily sludge and rice husks", International Journal of Hydrogen Energy, 47(64), pp. 27437–27451, 2022. https://doi.org/10.1016/j.ijhydene.2022.06.099

[27] Singh, S., Chakraborty, J. P., Mondal, M. K. "Pyrolysis of torrefied biomass: Optimization of process parameters using response surface methodology, characterization, and comparison of properties of pyrolysis oil from raw biomass", Journal of Cleaner Production, 272, 122517, 2020. https://doi.org/10.1016/j.jclepro.2020.122517

[28] Commandré, J.-M., Lahmidi, H., Salvador, S., Dupassieux, N. "Pyrolysis of wood at high temperature: The influence of experimental parameters on gaseous products", Fuel Processing Technology, 92(5), pp. 837–844, 2011. https://doi.org/10.1016/j.fuproc.2010.07.009

[29] Di Blasi, C., Branca, C. "Kinetics of Primary Product Formation from Wood Pyrolysis", Industrial & Engineering Chemistry Research, 40(23), pp. 5547–5556, 2001. https://doi.org/10.1021/ie000997e

[30] Gupta, S., Patel, P., Mondal, P. "Biofuels production from pine needles via pyrolysis: Process parameters modeling and optimization through combined RSM and ANN based approach", Fuel, 310, 122230, 2022.
https://doi.org/10.1016/j.fuel.2021.122230

[31] TIBCO Software Inc. "Statistica Software V12.5.192.7", [computer program] Available at: https://www.statistica.com/en/ [Accessed: 04 October 2022]

[32] Kumar, M., Mishra, P. K., Upadhyay, S. N. "Pyrolysis of *Saccharum munja*: Optimization of process parameters using response surface methodology (RSM) and evaluation of kinetic parameters", Bioresource Technology Reports, 8, 100332, 2019.
https://doi.org/10.1016/j.biteb.2019.100332

[33] Kumar, S., Singh, R. K. "Optimization of process parameters by response surface methodology (RSM) for catalytic pyrolysis of waste high-density polyethylene to liquid fuel", Journal of Environmental Chemical Engineering, 2(1), pp. 115–122, 2014.
https://doi.org/10.1016/j.jece.2013.12.001

[34] Sakthivel, R., Ramesh, K., Joseph John Marshal, S., Sadasivuni, K. K. "Prediction of performance and emission characteristics of diesel engine fuelled with waste biomass pyrolysis oil using response surface methodology", Renewable Energy, 136, pp. 91–103, 2019.
https://doi.org/10.1016/j.renene.2018.12.109

[35] Gupta, G. K., Mondal, M. K. "Bio-energy generation from sagwan sawdust via pyrolysis: Product distributions, characterizations and optimization using response surface methodology", Energy, 170, pp. 423–437, 2019.
https://doi.org/10.1016/j.energy.2018.12.166

[36] Dhanavath, K. N., Bankupalli, S., Sugali, C. S., Perupogu, V., V Nandury, S., Bhargava, S., Parthasarathy, R. "Optimization of process parameters for slow pyrolysis of neem press seed cake for liquid and char production", Journal of Environmental Chemical Engineering, 7(1), 102905, 2019.
https://doi.org/10.1016/j.jece.2019.102905

[37] Kılıç, M., Pütün, E., Pütün, A. E. "Optimization of *Euphorbia rigida* fast pyrolysis conditions by using response surface methodology", Journal of Analytical and Applied Pyrolysis, 110, pp. 163–171, 2014.
https://doi.org/10.1016/j.jaap.2014.08.018

[38] Wang, Z., Li, J., Barford, J. P., Hellgradt, K., McKay, G. "A comparison of chemical treatment methods for the preparation of rice husk cellulosic fibers", International Journal of Environmental & Agriculture Research, 2(1), pp. 67–77, 2016.

[39] Banks, S. W., Bridgwater, A. V. "14 - Catalytic fast pyrolysis for improved liquid quality", In: Luque, R., Lin, C. S. K., Wilson, K. Clark, J. (eds.) Handbook of Biofuels Production: Processes and Technologies, Woodhead Publishing, 2016, pp. 391–429. ISBN 978-0-08-100455-5
https://doi.org/10.1016/B978-0-08-100455-5.00014-X

[40] Li, G., Xiang, S., Ji, F., Zhou, Y., Huang, Z. "Thermal cracking products and bio-oil production from microalgae *Desmodesmus* sp.", International Journal of Agricultural and Biological Engineering, 10(4), pp. 198–206, 2017.
https://doi.org/10.25165/j.ijabe.20171004.3348

[41] Maher, K. D., Bressler, D. C. "Pyrolysis of triglyceride materials for the production of renewable fuels and chemicals", Bioresource Technology, 98(12), pp. 2351–2368, 2007.
https://doi.org/10.1016/j.biortech.2006.10.025

[42] Chen, G., Liu, C., Ma, W., Zhang, X., Li, Y., Yan, B., Zhou, W. "Co-pyrolysis of corn cob and waste cooking oil in a fixed bed", Bioresource Technology, 166, pp. 500–507, 2014.
https://doi.org/10.1016/j.biortech.2014.05.090

[43] Akalın, M. K., Tekin, K., Karagöz, S. "Hydrothermal liquefaction of cornelian cherry stones for bio-oil production", Bioresource Technology, 110, pp. 682–687, 2012.
https://doi.org/10.1016/j.biortech.2012.01.136

[44] Liu, Y., Yuan, X.-Z., Huang, H.-J., Wang, X.-L., Wang, H., Zeng, G.-M. "Thermochemical liquefaction of rice husk for bio-oil production in mixed solvent (ethanol-water)", Fuel Processing Technology, 112, pp. 93–99, 2013.
https://doi.org/10.1016/j.fuproc.2013.03.005

[45] Karagöz, S., Bhaskar, T., Muto, A., Sakata, Y. "Comparative studies of oil compositions produced from sawdust, rice husk, lignin and cellulose by hydrothermal treatment", Fuel, 84(7–8), pp. 875–884, 2005.
https://doi.org/10.1016/j.fuel.2005.01.004